Two electron interference in angular resolved double photoionization of Mg

E. Sokell[1], P. Bolognesi[2], A. Kheifets[3], I. Bray[4], S. Safgren[1] and L. Avaldi[2]

[1] School of Physics, UCD Science Centre, Belfield, Dublin 4, Ireland

[2] CNR-Istituto di Metodologie Inorganiche e dei Plasmi, Area della Ricerca di Roma1, 00015 Monterotondo Scalo, Italy

[3] RSPE, The Australian National University, Canberra ACT 0200, Australia

[4] ARC Centre for Matter-Antimatter Studies, Curtin University, WA 6845 Perth, Australia

corresponding author: lorenzo.avaldi@imip.cnr.it

Abstract. The signature of the target wavefunction has been observed in the symmetrized amplitude of the resonant double photoionization of Mg. This observation is based on our experimental study of angle-resolved double photoionization of Mg at the photon energy of 55.49 eV (2p $\rightarrow$3d resonance) under equal energy sharing conditions.

1. Introduction

There are processes characterized by differential cross sections, either in energy or in angle, which carry the signature of the target orbitals and therefore are used to extract information on the electronic structure in the gas phase as well as in condensed matter. Examples are the Cooper minimima [1-4] in the photoionization cross section determined by the vanishing radial overlap between the photoelectron wave function and the target orbital and the different shapes of the angular distribution in impulsive (e,2e) experiments, which are the kernel of the Electron Momentum Spectroscopy [5]. The situation is much more complicated in the case of double photoionization, DPI, and no simple analogue of the Cooper minimum exists. Nevertheless, a strong effect of the target electronic structure was observed in calculations of the angular correlation pattern in the two-electron continuum [6]. It has been shown that i) for a given symmetry of the electron pair the angular correlation of DPI mimics the angular distribution of an e-impact ionization of the corresponding ion and ii) the amplitudes of these processes are strongly determined by the radial extent and oscillations of the target orbital of the singly charged ion. In the case of the Cooper minimum, the contributions of the positive and negative oscillations of the target orbital cancel each other in the real and scalar quantity (the dipole radial integral). In the case of DPI, these contributions add up as complex and angular dependent amplitudes. They do not vanish entirely, but display an intricate interference pattern.

Alkaline-earth-metal atoms (Be, Mg, Ca, Sr) are "quasi two electron" systems with the outermost orbitals characterized by one or more nodes thus they represent the most suitable candidates to investigate these predictions. To the purpose we have undertaken an investigation of the DPI of Mg to $Mg^{2+}(3s^{-2})$ [7] and here we report some results in the equal energy sharing conditions at 55.49 eV.

2. Experimental

The experiments have been performed using the multicoincidence end-station [8] of the Gas Phase Photoemission beamline [9] at Elettra, where an undulator of period 12.5 cm, 4.5 m long produces fully linearly polarized radiation in the photon energy range 13-1000 eV. The vacuum chamber hosts two independent turntables, holding respectively three and seven electrostatic hemispherical analyzers spaced by 30° of each other. The three spectrometers of the smaller turntable, are mounted at 0°, 30° and 60° with respect to the polarization vector $\hat{\varepsilon}\|\hat{x}$ of the light in the plane (x,y) perpendicular to the direction $\hat{z}$ of propagation of the radiation. They have been used to measure the 'fixed electron', labeled 1. The larger turntable rotates in the same plane and its seven analyzers have been used to measure the angular distribution of the correlated electron, labeled 2. The ten analyzers have been set to detect electrons of kinetic energy $E_1 = E_2 = 16.4$ eV. The energy resolution and the angular acceptance were $\Delta E/E_{1,2} = 0.03$ and $\Delta\theta_{1,2} = \pm 3°$, respectively. The photon energy resolution was about 150 meV. The relative angular efficiency of the ten analyzers has been established by measuring the photoelectron angular distributions of Mg 2p and Ne 2p, with well known asymmetry parameters [10,11]. The metal vapour source is collinear with the photon beam, which passes through the hollow core of the source before interacting with the atomic beam and ending up on the photodiode, to be monitored. Six apertures drilled into the closure piece of the crucible and pointing to the interaction region increase the atom density at the interaction region. The oven has been operated at a temperature setting of 410 and 470° C for the bottom and top parts of the crucible, respectively. An independent hypodermic needle is used to admit rare gases in the interaction region for tuning and calibration purposes. An accumulation time of about 3 hours/point was necessary to reach the present accuracy in the experimental results.

3. Results and discussion

The experimental triple differential cross section (TDCS), $d^3\sigma / d\Omega_1 d\Omega_2 dE_1$ where $\Omega_i = (\theta_i, \varphi_i)$ (i=1,2) are the direction of emission of the two photoelectrons and E_1 the energy of one of the photoelectrons, the other being determined by energy conservation $h\nu - I^{2+} = E_1 + E_2$, are shown in figure 1. The measurements have been performed at 55.49 eV, which corresponds to the excitation of the $Mg(2p^6 3s^2) \rightarrow Mg(2p^5 3s^2 3d)$ resonance, because the measurement of the TDCS of metal vapours even at the third generation synchrotron radiation sources is very challenging.

The experiments have been compared with the prediction of the convergent close coupling model, CCC, [12] which cannot tackle resonant processes ab initio. Thus, to calculate the TDCS properly, the effect of the resonant excitation has been incorporated semi-empirically in the CCC formalism, as described in [7]. While, on one hand, the resonance enhances the photoabsorption cross section, on the other hand, it may affect the shape of the TDCS. In order to check this, two calculations, one including the resonant process and one without, have been performed. The absolute cross section for the non-resonant case is about a factor of four lower than in the calculations including the resonance. The comparison between non-resonant/resonant CCC calculations shows that the "resonance" does not introduce extra features in the TDCS, but does change the relative intensity of the lobes [7]. In figure 1 the calculations including the resonance are shown.

At all θ_1 the TDCS shape displays a node at the relative angle of emission of the two electrons, θ_{12}, of 180° as expected for the singlet odd character of the double continuum wave function. At $\theta_1 = 0°$ theory predicts two lobes of equal intensities, while at $\theta_1 = 30°$ and 60° the TDCS is mainly concentrated in one structure with some minor features: a small lobe at about 230° and a non-vanishing cross section at about 100° at $\theta_1 = 30°$, a series of three small lobes at $\theta_1 = 60°$. The quality of the data does not allow the complete resolution of all of these features, but the general trend is in fair agreement with the predictions. At all θ_1 the additional feature predicted in the main lobe, cannot be discerned in the experimental data. As far as the comparison with the double ionization of He for equal energy sharing at similar excess energy [6] is concerned, one sees that the Mg TDCS share with He the node at $\theta_{12} = 180°$, but the lobes in Mg are significantly narrower and the relative intensity and

number of minor lobes at θ_1= 30° and 60° are different. As the three TDCS were measured simultaneously, they can be reported on the same relative scale of intensity. A common scaling factor between theory and experiment has been used for the TDCS of Mg at θ_1=30° and 60°, while the theory appears to overestimate the experiment by a factor 2.2 at θ_1=0°. Similar variation of the scaling coefficients by a factor of 1.6 was required for He [7], which indicates the level of agreement between the present theory and experiment that we may expect.
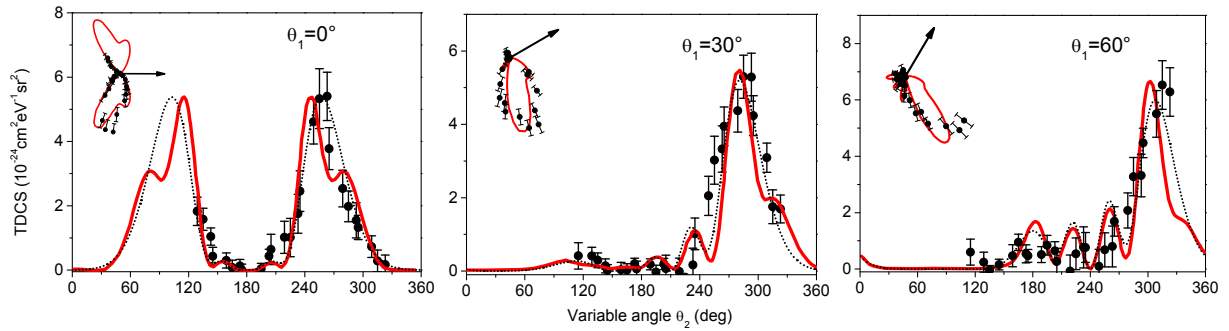

Figure 1. TDCS of Mg in equal energy sharing ($E_1=E_2=16.4$ eV) kinematics for three fixed reference angles θ_1=0°, 30° and 60°. The resonant CCC calculation is fitted with the di-Gaussian parameterization eq. (3) (black dot line). The experimental TDCS have been rescaled to the CCC calculations (full red curve) (see text).The polar plot of the TDCS are shown in the insets.

For equal energy sharing the TDCS is determined by the symmetric, or gerade, a_g amplitude [13]

$$TDCS(E_1,E_2,\theta_{12}) \propto \left| a_g(E_1,E_2,\theta_{12})(\cos\theta_1 + \cos\theta_2) \right|^2 \quad (1)$$

The Mg amplitude extracted from the experimental TDCS is shown with error bars in figure 2a, where it is also compared with the amplitude predicted by CCC. The comparison between the theoretical and experimental amplitudes is quite satisfactory, although the quality of the data hampers a clear observation of the predicted minimum in the amplitude.

Based on Wannier-type theories [14], in which the angular variation near the Wannier saddle decouples from the radial motion and can be described by the ground-state wave function of a harmonic oscillator, the symmetric amplitude a_g has been represented by a Gaussian function,

$$\left| a_g \right| = A\exp\left[-2\ln 2(\theta_{12}-180)^2 / \gamma^2\right] \equiv G(A,\gamma,\theta_{12}) \quad (2)$$

where γ is the correlation width. The Gaussian ansatz has been found to be a useful approximation to describe the symmetric amplitude of the double photoionization of He up to an excess energy of 80 eV [15]. The central portion of the Mg amplitude, near the mutual photoelectron angle θ_{12}=180°, can be represented by the Gaussian ansatz, but the fringes of the Mg amplitude cannot. Indeed, the whole of the Mg amplitude can be better described by the di-Gaussian parametrization proposed in [6]

$$a_g = G_1(A_1,\gamma_1,\theta_{12}) + e^{i\phi}G_2(A_2,\gamma_2,\theta_{12}) \quad (3)$$

The complex phase factor, ϕ, represents the interference of the two Gaussians. The five constants $A_{1,2}$, $\gamma_{1,2}$ and ϕ are used as fitting parameters. As was argued in [6], the Gaussian width may be linked to the radial extent of the target orbital of the singly charged ion. A sparser target orbital can be reached by a

larger number of partial waves of the electron in the continuum, which leads to a narrower Gaussian. Thus, it is natural to associate the wide and narrow Gaussians with two characteristic regions in the target coordinate space. In DPI of the 2s-shell atomic targets, these two regions are related to the positive and negative oscillations of the target orbital. In the present case of a 3s-shell target orbital, there are three oscillations but the first one, near the origin, is very small as is seen in Figure 2b, where the Mg 3s orbital is compared to the He 1s one, and hence will have a negligible contribution to the DPI amplitude.
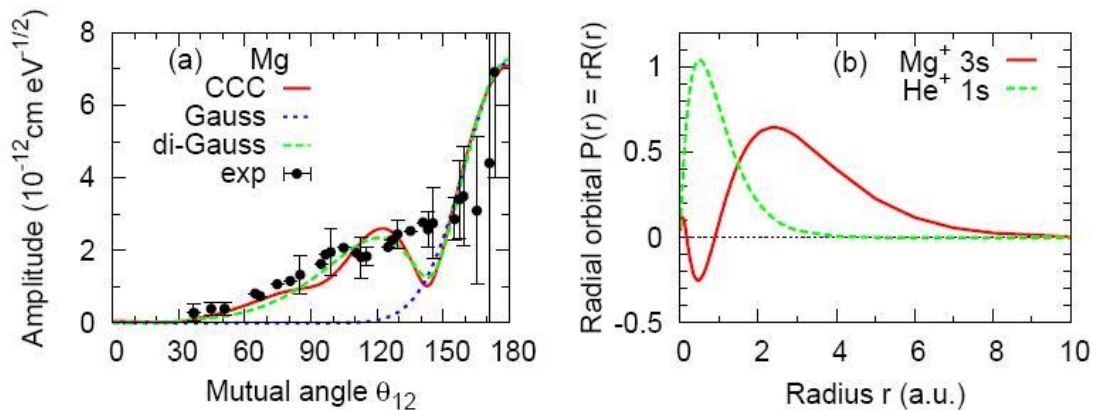

Figure 2. (*a*) The symmetric gerade amplitude of DPI of Mg at $E_1 = E_2 = 16.4$ eV is shown as a function of the mutual photoelectron angle θ_{12}. The CCC calculation (red solid line) is fitted with the Gaussian ansatz eq. (2) (blue dashed line) and di-Gaussian parameterization eq. (3) (green dashed line). The Mg amplitude extracted from the experimental TDCS is shown with error bars. (*b*) The radial orbitals $P(r) = rR(r)$ for Mg^+ 3s (red solid line) and He^+ 1s (green dashed line).

The di-gaussian function, eq.(3), has been fitted to the experimental data and CCC calculations. The obtained parameters for the experimental data (and the CCC calculations) are as follows: $A_2/A_1 = 0.42 \pm 0.08$ (0.43), $\gamma_1 = 30 \pm 2°$ (41.2), $\gamma_2 = 95 \pm 4°$ (89.2), $\phi = 133 \pm 5°$ (160). In comparison, the theoretical Gaussian width for He is 97° which is similar to the γ_2 parameter for Mg. This is consistent with the similar peak positions of the negative oscillation of the Mg^+ 3s orbital and the positive oscillation of the He^+ 1s orbital, as shown in figure 2b. The comparison between the theoretical and experimental di-Gaussian parameters is quite satisfactory. The experimental width γ_1 tends to be smaller than the predicted one.
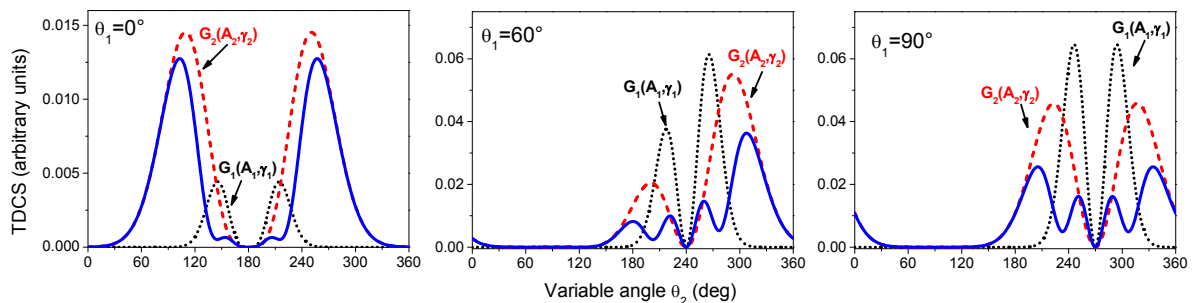

Figure 3. The TDCS obtained using the narrow (black dot line) and broad (red dash line) Gaussian functions and the di-Gaussian function (black solid line) at $\theta_1 = 0°$, 60° and 90°. The TDCS have been calculated using the parameters which provide the best fit to the CCC predictions (see text).

Even though the contribution of the broader Gaussian function, $G_2(A_2, \gamma_2, \theta_{12})$, to the amplitude is smaller than the one of the narrow Gaussian function, $G_1(A_1, \gamma_1, \theta_{12})$, its contribution to the TDCS is

actually dominant. This is shown in figure 3 where the TDCS obtained using the di-Gaussain correlation factor or the two Gaussian, $G_i(A_i, \gamma_i, \theta_{12})$ i=1,2, functions calculated using the parameters of the best fit to the CCC calculations at θ_1=0, 60 and 90°, are plotted separately. At θ_1=0°, almost all of the intensity of the TDCS comes from the broader Gaussian peak and almost none from the narrower one. The narrower Gaussian contribution becomes more significant at the other fixed angles, θ_1=60 and 90°, but the broader Gaussian contribution still dominates the TDCS. This behavior can be easily understood because the portion of amplitude at θ_{12}=180°, which corresponds to the back-to-back emission, is suppressed by the kinematic factor due to the dipole selection rules, while the contribution of the broader Gaussian function G_2, which is still large away from the kinematic node, is not damped. This is clearly shown in figure 4 where the di-Gaussian correlation and angular factors are overimposed on an arbitrary scale to TDCS calculated using the $G_1(A_1, \gamma_1, \theta_{12})$ and $G_2(A_2, \gamma_2, \theta_{12})$ functions.
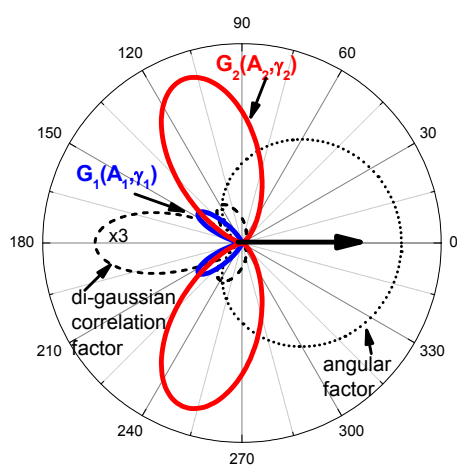

Figure 4. The contributions of the angular factor (black dot line) and the symmetrized gerade amplitude of eq. (1) (black dash line) for the TDCS at θ_1=0° overimposed to the TDCS calculated using the $G_1(A_1, \gamma_1, \theta_{12})$ (blu solid line) and $G_2(A_2, \gamma_2, \theta_{12})$ functions (red solid line). The parameters obtained by the best fit to the CCC calculations have been used.

This is the first experimental observation of a strong modification of the symmetric amplitude in the DPI of a *ns*-orbital with respect to the one of He. This modification is related to the structure of the radial wavefunction of the target orbital. It manifests itself in a non-Gaussian amplitude. This is similar to Cooper minimum in single photoionization cross section. However the weaker constraints on the angular momenta of the electron pair result in an interference pattern instead of a simple minimum. This interference is similar to the one of the electron "two-slit" experiments. There the wave functions of the electrons, "emitted" from different spatial positions, interfere. Here, similarly, the wave functions of two-electron pairs "originated" from two different regions of the charge density interfere. This effect is well described by a representation of the gerade amplitude by a di-Gaussian function. Just as the Cooper minimum is a universal phenomenon, the breaking down of the Gaussian ansatz in describing the symmetric DPI amplitude should be found in all quasi two-electron targets beyond helium.

References

[1] Fano U and Cooper J W 1968 *Rev. Mod. Phys.* **40** 441
[2] Bertrand J B *et al* 2012 *Phys. Rev. Lett.* **109** 143001
[3] Molodtsov S L *et al* 2001 *Phys. Rev. Lett.* **87** 017601
[4] Vyalikh D V *et al* 2008 *Phys. Rev. Lett.* **100** 056402

[5] Weigold E and McCarthy I E 1999 *Electron Momentum Spectroscopy* (Kluwer Academic/Plenum, New York)

[6] Kheifets A S, Bray I, Colgan J and Pindzola M S 2011 *J. Phys. B: At. Mol. Opt. Phys.* **44** 011002

[7] Sokell E, Bolognesi P, Kheifets A, Bray I, Safgren S and Avaldi L 2013 *Phys. Rev. Lett.* **110**, 083001 and 2013 *Phys. Rev. A* submitted

[8] Bolognesi P *et al* 2004 *J. Electron. Spectrosc. Rel. Phenom.* **141** 105

[9] Blyth R R *et al* 1999 *J. Electron Spectr. Rel. Phenom.* **101-103**, 959

[10] Soutworth S H, Parr A C, Hardis J E, Dehmer J L and Holland D M P 1986 *Nucl. Instrum. Meth. A* **246** 782

[11] Kämmerling B, Hausmann A, Laüger J and Schmidt V 1992 *J. Phys. B: At. Mol. Opt. Phys.* **25** 4773

[12] Kheifets A S and Bray I 2007 *Phys Rev. A* 75, 042703

[13] Avaldi L and Huetz A 2005 *J. Phys. B: At. Mol. Opt. Phys.* **38** S861

[14] Rau A R P 1976 *J. Phys. B: At. Mol. Opt. Phys.* **9** L283 , Feagin J M 1984 *J. Phys. B: At. Mol. Opt. Phys.* **17** 2433, Rost J M 1994 *J. Phys. B: At. Mol. Opt. Phys.* **27** 5923

[15] Kheifets A S and Bray I 2002 *Phys. Rev. A* **65** 022708